Anti-CXCR4 chemokine receptor, motixafortide, as an adjunct treatment with anti-TB drugs decreases the bacterial burden by improving drug distribution

KUSUMA SAI DAVULURI[1], AMIT KUMAR SINGH[1], AJAY VIR SINGH[1], VIMAL KUMAR[1], SHOOR VIR SINGH[2] and DEVENDRA SINGH CHAUHAN[1]

[1]Department of Microbiology and Molecular Biology, ICMR-National JALMA Institute for Leprosy and Other Mycobacterial Diseases, Agra 282001; [2]Department of Biotechnology, GLA University, Mathura 281406, India

Received August 29, 2022; Accepted January 2, 2023

DOI: 10.3892/wasj.2023.190

Abstract. C-X-C motif chemokine receptor 4 (CXCR4) is involved in the migration of bloodcells and the formation of blood vessels. It is expressed on blood cells and other immune cells such as dendritic cells and lymphocytes. *Mycobacterium tuberculosis* (*M.tb*) induces granuloma-associated angiogenesis, which is associated with the mycobacterial-induced expression of CXCR4. However, the significance of pathogen-induced angiogenesis remains elusive. The aim of the present study was to investigate the role and expression levels of CXCR4 during *M.tb* infection. To inhibit CXCR4, motixafortide, an antagonist for CXCR4, was used. The effect of motixafortide on *M.tb* dissemination, attenuation of bacterial growth and immunological responses in a guinea pig animal model was extensively studied using immunohistochemistry, as well as immunological and colony enumeration assays. The pharmacokinetics of first-line drugs in plasma, the lungs, and granuloma were evaluated following the inhibition of the expression of CXCR4 through motixafortide therapy. The results revealed that CXCR4 stimulation induced the expression of vascular endothelial growth factor-A (VEGFA) in *M.tb*-infected guinea pigs. Improvement in the pharmacokinetic parameters and early bacterial clearance in the spleen were observed in motixafortide anti-tuberculosis (TB) drug therapy in contrast to therapy with first-line drugs alone. G ranulomatous capture of first line drugs combined with motixafortide may have significant implications through different mechanisms. In the present study, it was demonstrated that CXCR4 inhibitors may be used as a therapeutic strategy to combat granuloma-angiogenesis by interfering with VEGFA signalling and controlling the spread of *M.tb* infection.

Correspondence to: Dr Devendra Singh Chauhan, Department of Microbiology and Molecular Biology, ICMR-National JALMA Institute for Leprosy and Other Mycobacterial Diseases, Dr Myazaki Street, Tajganj, Agra 282001, India
E-mail: devchauhan01@yahoo.co.in; 604dks@gmail.com

Key words: pharmacokinetics, vasculature, motixafortide, chemokine receptor, dissemination

Introduction

Tuberculosis (TB) is a contagious infection caused by *Mycobacterium tuberculosis* (*M.tb*) that most often affects the lungs. In 2020, 4.9 million cases of TB were reported, down from 6.3 million the year before. This indicates that in 2020, 1.4 million individuals did not receive treatment for TB (1). Dissemination of *M.tb* occurs from the lungs of the host to peripheral sites for antigen specific T-cell mediated immunity. The potential of *M.tb* to disseminate through the bloodstream and lymph has been confirmed. As a result, TB has been reported practically in all tissues and organs (2). Extrapulmonary TB accounts for ~20% of all TB cases in immunocompromised patients, and in HIV-infected individuals it is diagnosed in ~50.0% of the cases (3). Despite this data, research on miliary TB is limited, possibly due to the difficulty in diagnosis and issues related to biopsy collection. During TB infection, the host triggers an immune response that eliminates the bacteria in a dense cellular mass called granuloma (4). The origin of new blood vessels induced during the infection plays a salient role in the spread of infection and restricts the penetration of anti-TB drugs from the blood to lesions containing mycobacterial cells (5,6). Infected macrophages often migrate from granulomas to tissues (7). A previous study demonstrated that granuloma structures with high vascularization and excess endothelial cells result in impaired blood flow to the granuloma sites and compromise drug delivery (8). This pathogenic vasculature limits the drug concentration in the granuloma, resulting in a severe bacterial burden. Chemokines play a predominant role in directing immune cells to inflammatory sites that may lead to unregulated angiogenesis and could be used to control disease severity (9-12). C-X-C motif chemokine receptor 4 (CXCR4) supports the migration of leukocytes to the inflammation site and their levels correspond with the degree of inflammation (13,14). CXCR4 signalling induces the expression of vascular enodthelial growth factor (VEGF), regulating morphogenesis, angiogenesis, and immune response (15-17). Motixafortide treatment was revealed to significantly reduce

the growth of human leukaemia and myeloma xenografts. Treatment with motixafortide specifically was demonstrated to trigger CXCR4-dependent apoptotic cell death in tumors. Animals treated with motixafortide exhibited smaller tumour sizes and weights, and larger necrotic areas (18). In this previous study, it was demonstrated that blockade of CXCR4 induced a difference in the infection burden due to impaired angiogenic support of granuloma formation. A chemokine antagonist blocks selective chemokine receptors that are disease-relevant and indispensable for disease progression. A previous study revealed the effect of CXCR4 inhibition on VEGF expression and T-cell infiltration (19). When combined with chemotherapy, motixafortide may enhance the benefits of first-line drug therapy. The aim of the present study, was to demonstrate that inhibiting CXCR4 may suppress the induction of an angiogenic programme in granulomas. Cellular migration and recruitment of cells to the infected areas may not be altered in *M.tb*-infected motixafortide-treated groups compared with *M.tb*-infected untreated groups. The findings of the present study indicated that blockade of CXCR4 reduces the abnormal vasculature, increases drug absorption at the granuloma, and reduces the spread of infection to other organs.

Materials and methods

Ethical statement. When conducting the animal research, all procedures were carried out in accordance with the guidelines and instructions of ARRIVE (https://arriveguidelines.org/). The experiments involving the use of guinea pigs were approved by the Institutional Animal Ethics Committee of the National JALMA Institute for Leprosy and Other Mycobacterial Diseases (NJIL & OMD; Agra, India). Lala Lajpat Rai University of Veterinary and Animal Sciences (Hisar, India) provided healthy out-bred Hartley strain male guinea pigs, aged 3-4 weeks (~350 g in weight). All the animal experimental methods described in the present study were conducted according to the relevant guidelines and regulations for handling laboratory animals and were approved (approval no. NJIL&OMD-3-IAEC/2019-08) by the Institutional Animal Ethics Committee of NJIL & OMD.

M.tb infection and drug treatment. The *M.tb* H37Rv strain, commonly used for animal infection studies at the laboratory of the authors (20), was cultured in Middlebrook 7H9 medium supplemented with 10% albumin dextrose catalase (ADC; both Difco Laboratories, Inc.; BD Biosciences) at 37˚C. The culture type of the mid-log phase was established, and aliquots were frozen at -70˚C until needed. Before usage, cultures were diluted in sterile normal saline and the bacterial concentration was set to $1x10^6$ cfu/ml.

Guinea pigs were aerosol-infected with the *M.tb* H37Rv strain using a Glas-Col full-body inhalation exposure device (Glas-Col LLC) calibrated to deliver ~150 colony-forming units (CFU) to the lungs (21). The animals were housed in cages in biological safety level 3 facilities for 10-11 weeks to allow pathological symptoms to develop. According to the Guide for the Care and Use of Laboratory Animals (22), ventilation was provided. Dry bulb room temperature (20-26˚C) was maintained to avoid the stress and strain from heat or cold conditions. Guinea pigs were maintained under specific-pathogen-free conditions with 30-70% relative humidiy. To ensure a normal diurnal cycle time, a controlled lighting system was used. The animals were provided with water and standard feed *ad libitum* as per the aforementioned guidelines.

A total of 35 animals were randomly allocated to seven groups (Table I) and administered 10 μg/kg of motixafortide, a CXCR4 antagonist with an IC_{50} value of 1 nM (MedChemExpress) by slow intraperitonal infusion as per the recommended protocol. Guinea pigs were injected with motixafortide subcutaneously thrice/week for 2 weeks after the established infection with the *M.tb* H37Rv strain. First line drugs, rifampicin and isoniazid (MilliporeSigma), 25 and 10 mg/kg, respectively, were administered orally following the early stage of *M.tb* infection for 5 days/week for 2 weeks. In guinea pigs, *M.tb* infection usually appears during the 4th week, which is considered an early infection (23). The animals were sacrificed at the 4th and 6th week pre-decided time points based on the drug treatment. The duration of the experiment was 8 weeks. Animals were monitored daily and no adverse events requiring euthanasia/death of the animals were reported during the experiments. All animal welfare factors were taken into account, including measures to reduce pain and discomfort through the use of anaesthesia and particular housing conditions. None of the animals succumbed during the whole experiment. For the assessment of the bacterial burden from low-dose aerosol infection, two guinea pigs were sacrificed following dissection and organ harvesting. Guinea pigs were anaesthetized with 4-5% isoflurane for induction and 1-2% for maintenance. Carbon dioxide (CO_2; volume displacement, 30-70% vol/min) method was used for euthanasia of guinea pigs. Blood was collected (3-5 ml) from heart under anaesthesia. During the 6th week, blood was collected 45-60 min after treatment. The death of the guinea pigs was verified by observing the cardiac activity.

Determination of bacterial counts. Bacterial burdens in the lungs and spleen of infected guinea pigs were determined at the 4th and 6th weeks of infection, respectively. Organs were weighed and homogenized in PBS. Tenfold serial dilutions of organ homogenates were plated on Middlebrook 7H10 (BD Biosciences) agar plates containing 10% OADC (BD Biosciences) and incubated at 37˚C for 21 days. Colonies on plates were manually enumerated for bacterial burden determination.

Segmentation of caseating granulomas and fractal analysis. Lungs and spleen tissues were collected from sacrificed animals, and the dissected lungs and spleen of guinea pigs were fixed in 10% buffered formalin to avoid putrefaction and autolysis of tissue specimens and also preserved in RNA for subsequent analysis, for routine histopathological examination and IHC analysis. Tissues that had been fixed in 10% buffered formalin for 48 h at 20-22˚C were extracted and stored in cassettes before being sent to a tissue processor. The specimens were dehydrated in an escalating sequence of alcohols, cleaned in xylene, and then embedded in paraffin wax in the tissue processor. The tissue processor was programmed to maintain the specimens in each chamber for the specified amount of time (Table II).

Table I. Basic experimental scheme.

Group	Treatment
Healthy	-
Infection	150-200 CFU of *M. tuberculosis strain* by aerosol inhalation on day zero (infection),estimation of CFU at designated time points i.e., 4th and 6th week of infection.
Treatment group: Motixafortide at 10 μg/kg, INH at 25 mg kg^{-1} and RIF at 10 mg kg^{-1} respectively, by oral gavage. The 4th week (acute stage), 8th week (chronic stage) and INH + RIF chemotherapy.	
Infection control 4th week (Treatment initiation: 2 weeks post-infection)	Infection: Treatment started at 2 weeks post-infection; daily administration of motixafortide for an additional 2 weeks. Estimation of CFU following a wash-out period of 3 days.
Infection control 6th week (Treatment initiation: 4 weeks post-infection)	Infection: Treatment started at 4 weeks post-infection; daily administration of motixafortide for an additional 2 weeks. Estimation of CFU following a wash-out period of 3 days.
Infection + anti-TB drugs (Chemotherapy initiation: 4 weeks post-infection)	Infection: Treatment started 4 weeks post-infection; daily administration of INH + RIF for an additional 2 weeks. Estimation of CFU following a wash-out period of 3 days.
Infection + anti-TB drugs + motixafortide (Chemotherapy initiation: 4 weeks post-infection)	Infection: Treatment started 4 weeks post-infection; daily administration of RIF + INH + motixafortide for an additional 2 week.s Estimation of CFU following a wash-out period of 3 days.

INH, isoniazid; RIF, rifampicin; CFU, colony-forming units; TB, tuberculosis.

Table II. Processing of specimens in the tissue processor.

Procedural aspects	Reagent	Duration (h)	No. of changes (per hour)
Dehydration in ascending grades of alcohols	70% ethanol	1	1
	80% ethanol	1	1
	90% ethanol	1	1
	Absolute alcohol	1	2
Alcohol removal and clearing of dehydrated tissue	Xylene	1	2
Paraffin wax embedding (or impregnation)	Paraffin wax with ceresin	1.30	2
		1.30	1

Sections (thickness, ~3-5 mm) were cut with a rotator microtome after trimming of the paraffin blocks of the tissue samples. The tissue ribbons obtained were floated onto a water bath at 50˚C and then placed onto silane-coated glass slides. The slides were placed on a hot plate at a temperature <50˚C for 30 min to remove residual moisture and maintain the sections firmly adherent. The slides were either stained or stored for subsequent staining. Prior to use, tissue sections on silane-coated slides were maintained at 60˚C for 2 h on a hot plate to dispel any residual moisture and to achieve maximum tissue adhesion. Sections (5 mm) from paraffin-embedded tissues were de-waxed and stained with haematoxylin and eosin (H&E) at room temperature, 20-25˚C for 3-5 min, as previously described (24) and observed under an Olympus CX43 (Olympus Corporation) light microscope for histological evaluation and to visualise bacteria in the surrounding tissues. All the necrotic lesions of the granuloma were manually delineated and lacunarity was observed through an Olympus BX51 (Olympus, Japan) light microscope using MagVision software (Magnus Opto Systems India Pvt., Ltd.). Regions of interest were drawn in images. Segmentation of the necrotic area was performed and was loaded into ImageJ software (version 1.53m; National Institutes of Health). The fractal area was measured using the box counting method. Fractal dimensions were calculated and averaged for mean values. The mean values of all necrotic regions of different groups were calculated and were used in further analysis.

mRNA profiling and quantification of chemokine transcripts. mRNA extraction was performed from the serum samples using the TRIzol-C (Sisco Research Laboratories Pvt., Ltd.) as per the manufacturer's protocol. The resulting RNA quantification was performed using NanoPhotometer NP-80 (Implen U.K.). RNA integrity was evaluated by agarose gel electrophoresis.

Reverse transcription-quantitative polymerase chain reaction (RT-qPCR) was performed using SuperScript™ III One-Step RT-PCR System with Platinum™ Taq DNA Polymerase (cat. no. 12574018) and SYBR Green detection kit (Roche Diagnostics) and signals were detected using Bio-Rad CFX-96 real-time thermal cycler. The primers were designed using Primer3Plus software (https://www.primer3plus.com/), and the sequences are presented in Table III. Each reaction was performed in triplicate for each animal with 0.2 mmol/l of each primer and 50 ng of cDNA template. The cycling conditions were as follows: Reverse transcription at 50˚C for 15 min, followed by 3 min of initial denaturation at 95˚C, 40 cycles of denaturation at 95˚C for 10 sec, and 30 sec of annealing/extension at 60˚C. Gene expression was normalised using the reference gene, GAPDH. Analysis of the relative gene expression data was performed using the $2^{-\Delta\Delta Cq}$ method as previously described (25).

Detection of VEGFA expression in lung tissue sections using fluorescence microscopy. Dewaxing was carried out by maintaining the tissue sections in a hot air oven for 20 min at a temperature of 60-65˚C or until melting of the wax. Rehydration was performed in four descending grades of alcohol (absolute alcohol, 90, 80 and 70% alcohol) and finally in distilled water, with each change 5 min. Antigen retrieval through sodium citrate buffer was then performed as previously described (26). This buffer was pre-heated until the temperature reached 90˚C and the slides were immersed in this buffer for 1 h in the water bath. The slides were allowed to cool at room temperature for 20 min. The slides were then washed in PBS for 5 min. Quenching was performed by treating the tissue sections with a solution of 2 ml of 30% H_2O_2 in 100 ml methanol for 20-30 min (0.6% H_2O_2 in methanol). Each section was then washed for 5 min with PBS. Following digestion using 500 μg pepsin/0.2 N HCl, for 30 min at 37˚C in a waterbath, post-fixation was performed using glycine followed by 4% paraformaldehyde for 20-30 min at room temperature. Subsequently, 5% bovine serum albumin (MilliporeSigma™) was used for blocking at 37˚C for 1 h. For fluorescence immunostaining with DAPI counterstain, AssayLite™ Mouse anti-VEGF antibody was used in conjunction with IgG-FITC-conjugated clone (AP70032) (cat. no. 70032-05141; Assaypro LLC) for 1 h at 37˚C. The tissue sections were incubated with the anti-VEGF antibody at a dilution of 1:100. Excess antibody was removed by washing with phosphate-buffered saline (PBS) at room temperature, and sections were then incubated with the secondary detection antibody (Invitrogen™ cat. no. G21040, lot no. 2359138; Thermo Fisher Scientific, Inc.), goat anti-mouse conjugated to HRP at a dilution of 1:1,000 at 37˚C for 1 h. End product visualisation was achieved via a fluorescence microscope using DAPI (Sisco Research Laboratories Pvt., Ltd.) for 15-20 min at 37˚C as the counter fluorescent stain.

Quantification of drug concentration and analytical conditions. Plasma was separated from the blood samples collected from the animal experiments. Plasma, up to 1 ml, was separated and stored at -80˚C. Concentrations of rifampicin and isoniazid were detected by following the recommended protocol (27,28). Analysis was performed on the High Performance Liquid Chromatography, Alliance 2996 system (Shimadzu Corporation) and separation was carried out using a C18 column (150 mm). The sample volume was 150 μl and the flow rate was 4 ml/min. The mobile phase consisted of water: methanol [60:40 (v/v)] containing perchloric acid and tetrabutyl n-ammonium hydroxide. The temperature was maintained at 25-28˚C throughout the analysis. Based on the pharmacokinetic variables such as peak concentration (C_{max}) and area under the concentration-time curve (AUC_{0-12}), the plasma concentration of the drugs was calculated using STATA 15.0 (StataCorp LLC).

Table III. Sequences used for reverse transcription-quantitative PCR.

Primers	Sequences (5'-3')	Melting temperature (˚C)
VEGFA	F: GGCCCATCGAGATGCTAGTG	60
	R: GCCCACAGGGATTTTCTTGC	60
GAPDH	F: ACCACAGTCCATGCCATCAC	60
	R: TGTCGCTGTTGAAGTCA	60
CXCL-12	F: CCTGCCGCTTCTTTGAGA	55
	R: CCTGGATCCACTTCAGCTTC	55
CXCR4	F: GTGATCTCTGCGACTGGCTT	60
	R: CACGAGTTTGCGCGATTAGG	59

VEGFA, vascular endothelial growth factor-A; F, forward; R, reverse.

Calculation of pharmacokinetic variables and statistical analysis. Each experiment was carried out in triplicate and outcomes were further assessed. Graphpad Prism 9 (GraphPad Software, Inc.) and Origin 2020 (Originlab Corporation) were used for statistical analysis. ImageJ/Fiji software version 1.53 m (National Institutes of Health) was used to measure VEGFA expression. The differences in CFU counts, VEGFA expression and RT-qPCR results across the groups were analyzed using GraphPad Prism 9 and statistically assessed using Bonferroni post hoc test with ANOVA to compare the mean of multiple groups and an unpaired t-test for comparisons between two groups. $P \leq 0.05$ was considered to indicate a statistically significant difference. The normal distribution (Gaussian) was interpreted through Shapiro-wilk test, Kolomogorov-Smirnov test, D'Agostino-Pearson test, Anderson-Darling test using GraphPad Prism 8. The HPLC data was assessed using Shapiro-Wilk test and it was determined that the data followed a normal distribution (alpha=0.05). The CFU data also assessed with the Shapiro-Wilk test exhibited a normal distribution (apha=0.05). Similar findings were noted for the remaining results (alpha=0.05; Shapiro-Wilk test), however N was too small to show statistical significance.

Results

CXCR4-induced angiogenesis permits M.tb to disseminate. It was observed that treatment with motixafortide in guinea pigs

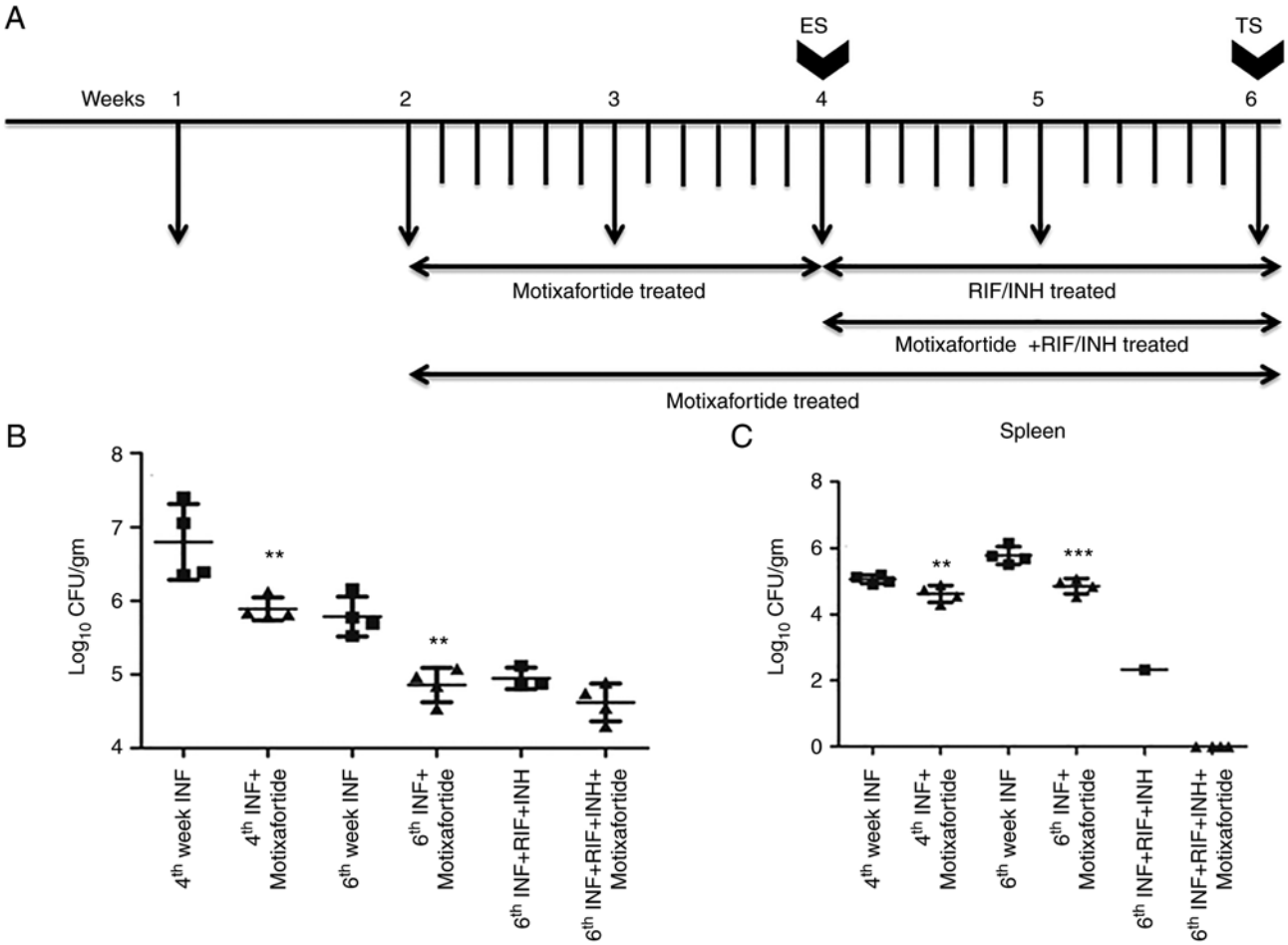

Figure 1. In guinea pigs, motixafortide improves the anti-TB activity of the first-line regimen. (A) Shematic diagram describing the therapeutic time period. Small lines indicate the number of days. (B) When compared to the control, motixafortide 10 μg/kg administered alone after 2 weeks of aerosol infection had a significant effect on the course of acute infection in lungs. When combined with rifampicin/isoniazid and motixafortide the lung bacillary load was markedly reduced compared to conventional therapy alone but not significantly. The results are shown as the mean $\log_{10}$CFU/g of (B) lungs and (C) spleen from five animals per group, at each time point, or as the proportion of lung exhibiting inflammatory involvement. The statistical comparison between groups was carried out using one-wayANOVA. Notably, not a single colony was found in the spleen of anti-motixafortide-treated guinea pigs. **P≤0.01 and ***P≤0.001 vs. 4th week INF or 6th week INF. TB, tuberculosis; RIF, rifampicin; INH, isoniazid; ES, early stage; TS, terminal stage; INF, infection.

for 2 weeks before the start of treatment did affect mycobacterial survival in the lungs and spleen compared to infected non-treated animals. After 4 weeks of infection, treatment with anti-TB drugs was initiated while motixafortide injections were continued along with the anti-TB drugs. The combination of 10 mg/kg rifampicin and 10 mg/kg isoniazid administered five times weekly for two weeks revealed potent bactericidal activity and lung CFU decreased from 6.8 log10 to 2.9 log10 CFU. However, the treatment with motixafortide reduced mycobacterial migration to distant organs, i.e., the spleen. Combination treatment with anti-TB drugs further reduced the mycobacterial migration and survival in the spleen, and the reduction was more than 2.1 log10 CFU compared to treatment with anti-TB drugs alone (P≤0.001; Fig. 1).

Treatment with motixafortide as an adjunct to anti-TB drugs increases the drug levels at the granuloma site. In plasma, lung and granuloma, RIF and INH were assessed concurrently after extraction. Analysis was performed using a C18 column at a wavelength of 267 nm. The retention times of rifampicin and isoniazid were 3 and 5.5 min, respectively (data not shown). Motixafortide treatment improved the drug delivery in granulomas. M.tb lesions on the lungs were isolated from the right apex region and caudal lung tissue was collected for drug assessment. Normalization of vasculature and refining the vascular perfusion increased the distribution of first line drugs in granulomas. Anti-CXCR4 treatment normalized the granuloma vasculature and, it was investigated whether the drug delivery can be improved by reducing the thickness of vascularity. Rifampicin and isoniazid delivery to TB lesions after 10 doses of anti-CXCR4 treatment compared with the controls was significantly higher (P<0.05; Fig. 2).

Expression levels of angiogenic genes elevated in M.tb-infected guinea pigs are reduced through motixafortide treatment. In order to understand the effect of CXCR4 inhibition by motixafortide, the expression of all ELR$^+$ chemokine ligands was determined. Significant changes in the expression of the CXCL12/CXCR4 axis and VEGF-A, which were increased following *M.tb* infection were also associated with angiogenesis. CXCL12 and CXCR4 mRNA expression were

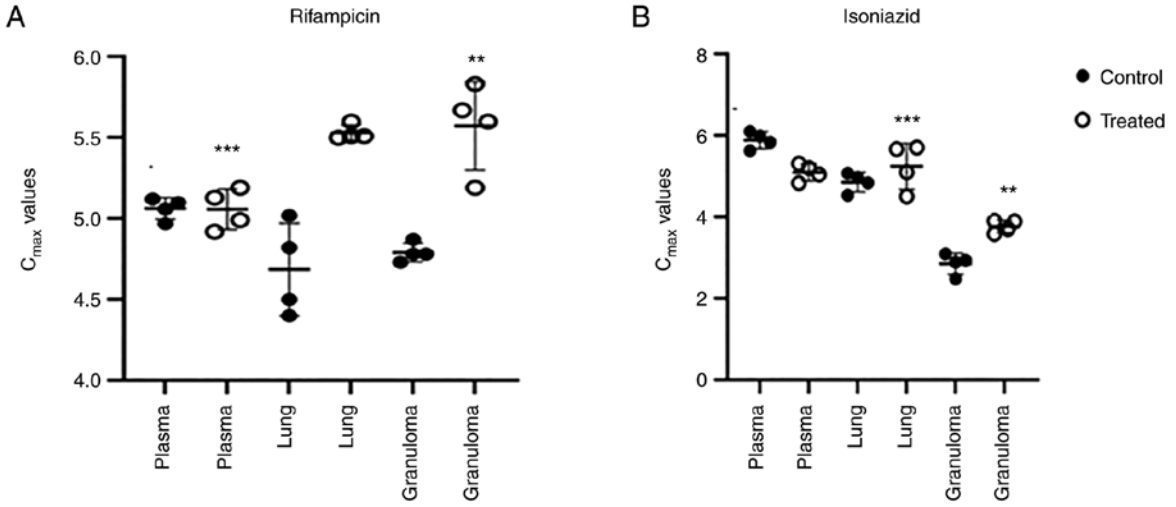

Figure 2. Motixafortide-treated guinea pigs combined with first-line drugs showed the effective penetration of drugs into the lesions. In plasma, no significant differences in isoniazid concentrations were observed. In plasma and granuloma significant differences were observed with rifampicin concentration. $^{**}P\leq0.01$ and $^{***}P\leq0.001$ vs. the control. C_{max}, peak concentration.

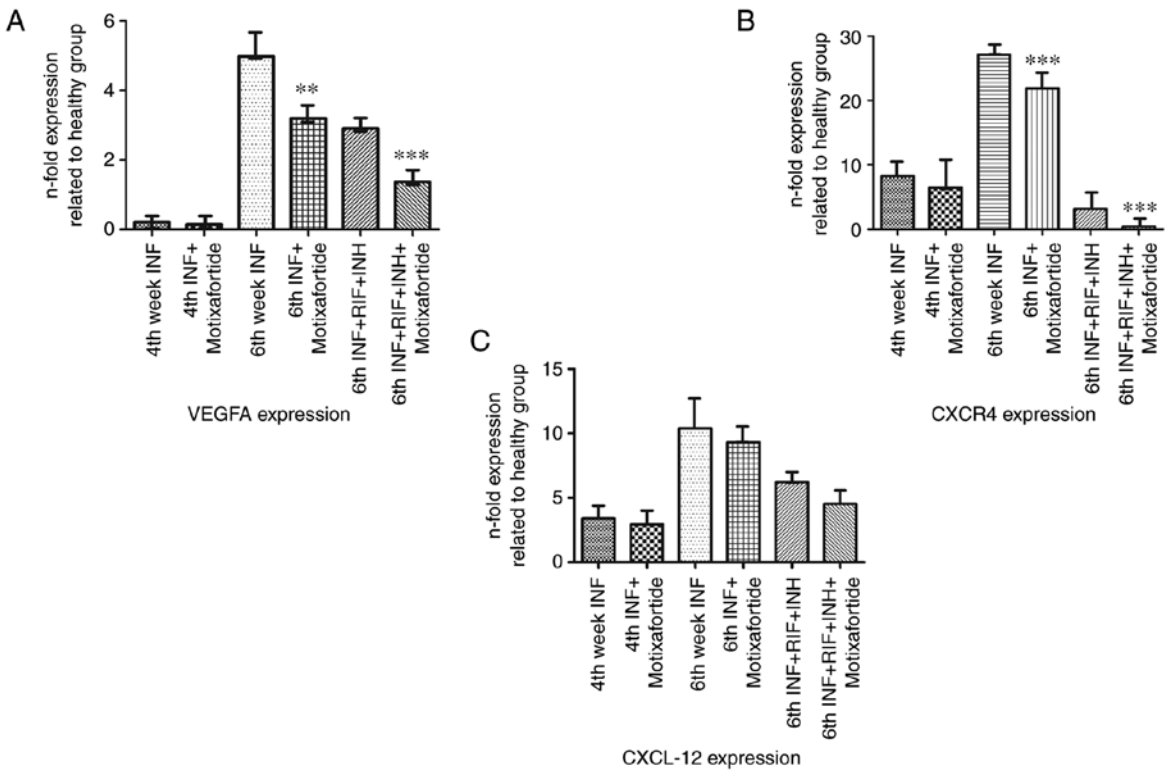

Figure 3. Expression levels of VEGFA, CXCR4 and CXCL-12. (A) Bar charts showing the levels of VEGFA in different groups. A one-way ANOVA multiple comparisions was used to compare the treated conditions to the infection control. The motixafortide-treated group at the 6th week exhibited a significant reduction in VEGFA levels when compared with the infection group and anti-TB drug treatment alone. (B) Bar charts showing the CXCR4 levels in different groups, revealed enhanced expression of CXCR4 in infected guinea pigs. Following motixafortide therapy, CXCR4 levels were significantly decreased. (C) Following *M. tb* infection, an increase in the CXCL-12 profile from 4th-week infection to 6th-week infection groups was revealed but no significant changes in CXCL-12 expression were revealed with motixafortide treatment ($P\geq0.01$, based on one-way ANOVA; n=5). $^{**}P\leq0.01$ and $^{***}P\leq0.001$ vs. 6th week INF or 6th week INF + RIF + INH. VEGFA, vascular endothelial growth factor-A; CXCR4, C-X-C motif chemokine receptor 4; *M. tb*, *Mycobacterium tuberculosis*; TB, tuberculosis; RIF, rifampicin; INH, isoniazid.

significantly increased in the lungs of guinea pigs infected with *M.tb*. Treatment with motixafortide significantly reduced the expression of the CXCL12/CXCR4 axis ($P<0.05$). Treatment with anti-TB drugs attenuated the mRNA level of CXCL12/CXCR4, which was further reduced in guinea pigs treated with anti-TB drugs and motixafortide combination. Similar results were observed for VEGF-A, where a combination of motixafortide and anti-TB drugs significantly reduced VEGF-A compared to anti-TB drugs alone, bringing the levels of angiogenic factors to a normal level (Fig. 3).

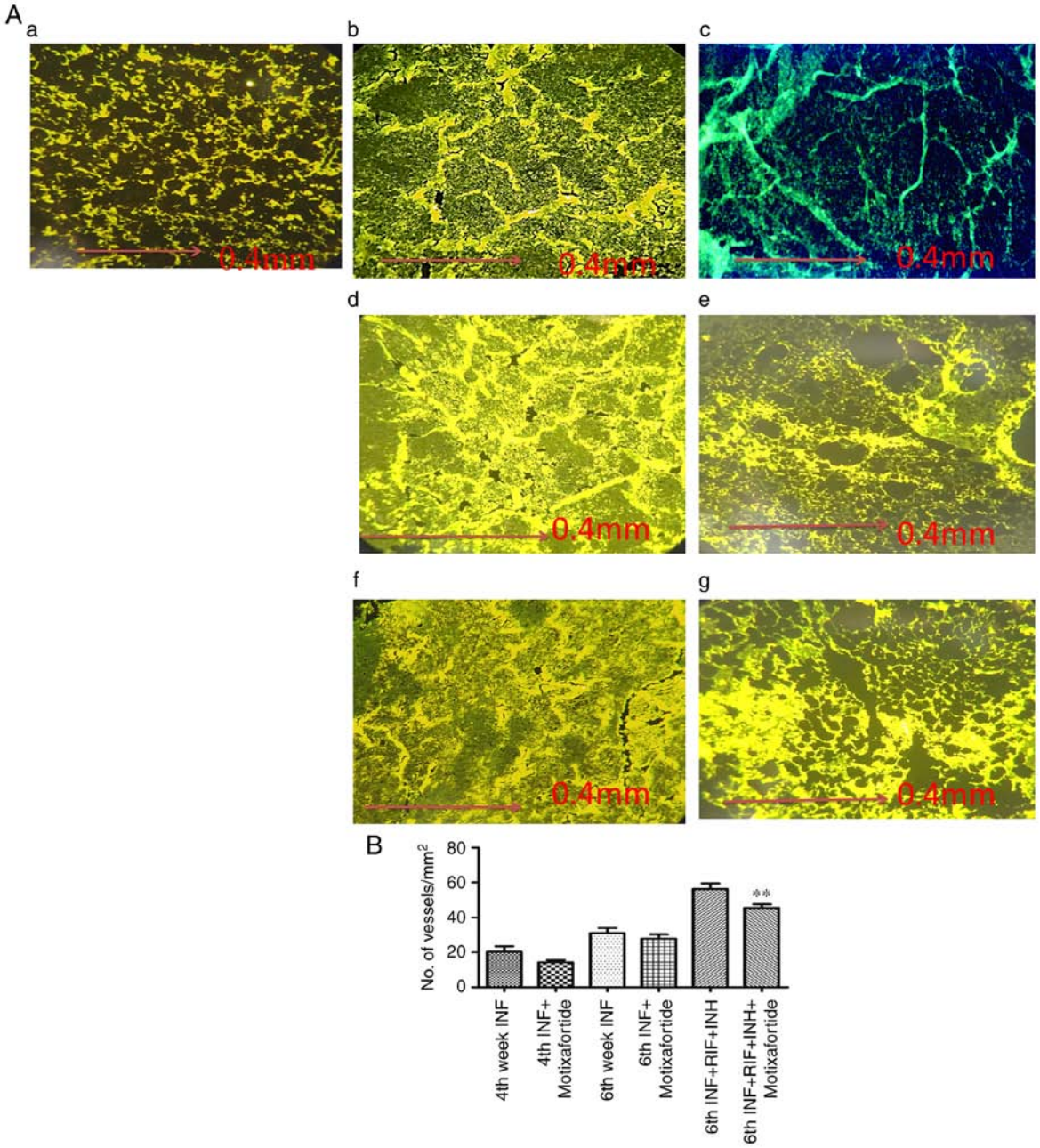

Figure 4. (A) Immunofluorescence-stained slides showing the expression of VEGFA in different groups (magnification, x40). A one-way ANOVA multiple comparisons was used to compare the treated conditions to the infection control. (a) Vascularity in the lungs was normal in the healthy guinea pigs. (b) VEGFA expression was significantly upregulated in 4th week of *M.tb*-infected guinea pig lungs. (c) Treatment with motixafortide for 2 weeks reduced the expression of VEGFA but not significantly. (d) VEGFA expression was markedly upregulated at the 6th week when compared with the 4th week. (e) Treatment with motixafortide for 4 weeks reduced the expression of VEGFA but not significantly. (f) Treatment with anti-TB drugs RIF + INH. (g) Treatment with anti-TB drugs and motixafortide combination. (B) Similar results were observed for VEGF mRNA expression. VEGF expression was significantly decreased after treatment with motixafortide Infection ($^{**}P \leq 0.01$ vs. 6th week INF + RIF + INH). The number of vessels was calculated per 3 microscopic fields and the graph was plotted. VEGFA, vascular endothelial growth factor-A; *M. tb*, *Mycobacterium tuberculosis*; TB, tuberculosis; RIF, rifampicin; INH, isoniazid.

CXCR4 inhibition reduces VEGFA expression. The vasculature was visualised in the lung tissues. Varied vascular morphologies were observed in the different groups of guinea pigs (Fig. 4Aa-g). The vessel thickness was measured and plotted (Fig. 4B). Motixafortide treatment had no effect on the microvessel density of granulomas in guinea pig tissue sections. However, there was a reduction in the thickness of the vessels. VEGF expression was considerably high in the affected regions of the lung tissue. The number of vessels was not affected by anti-CXCR4 treatment. It was observed that vessels associated with the internal region of the granulomas at the caseating region were collapsed, which was normalised through anti-CXCR4 treatment. Treatment with anti-TB drugs attenuated the level of VEGFA which was further reduced in guinea pigs treated with anti-TB drugs and motixafortide combination respectively (Fig. 4).

CXCR4 impairment reduces granulomatous necrotic regions. The necrotic core was markedly evident by the 4th week, which appears to indicate the development of a necrotic region before

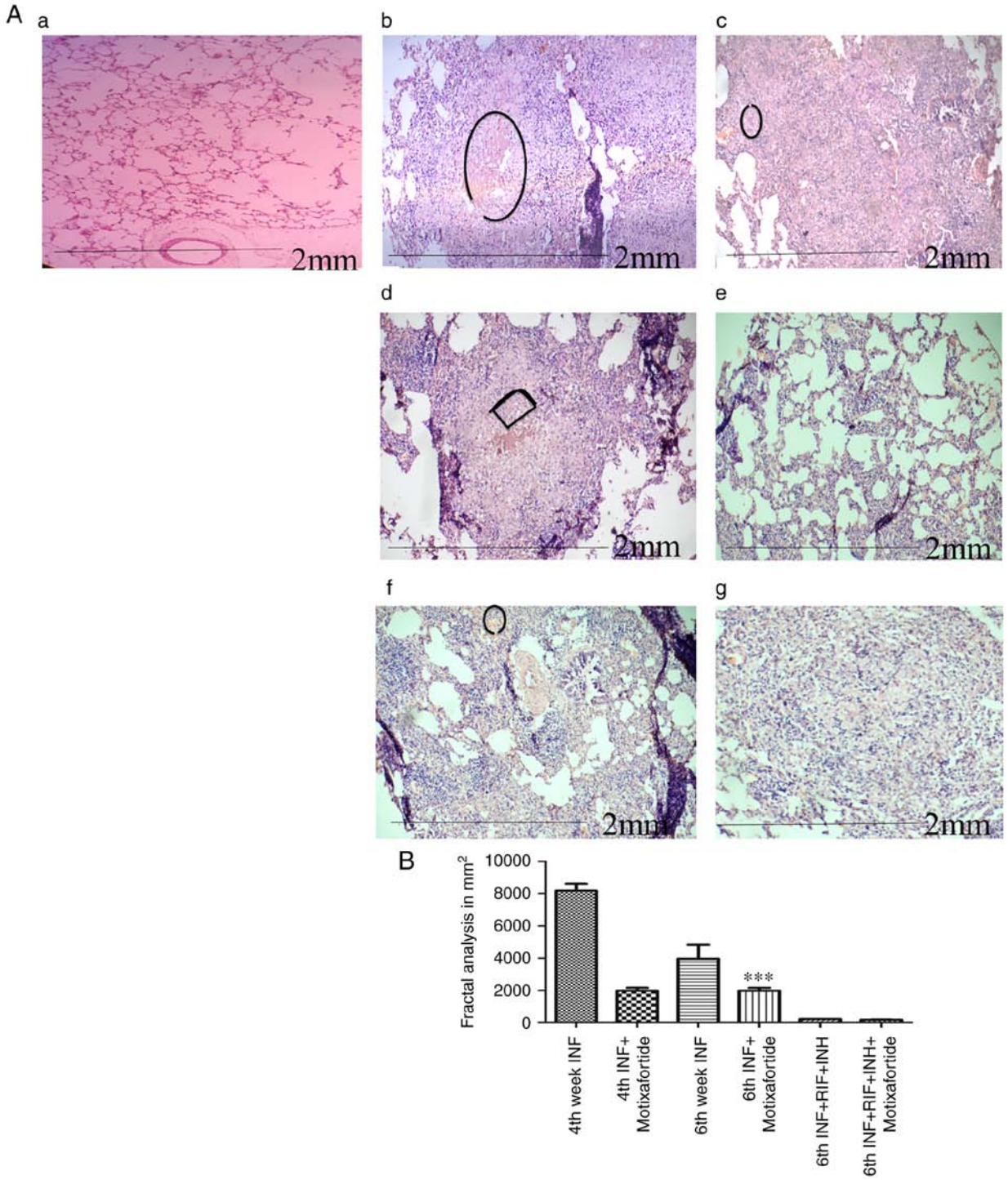

Figure 5. (A) H&E stained slides showing the necrotic area. Central core of the caseating granulomas of primary tuberculosis was observed surrounded by lymphocytes and macrophage cells in blue colour (magnification, x40). (a) Healthy guinea pig lung tissue sections. (b) During the 4th week infection in the guinea pigs the necrotic area in lung granulomas is shown. (c) Motixafortide-treated *M.tb*-infected guinea pigs exhibited a reduction in the necrotic regions. (d) Deconstructed granuloma was observed during the late stage of *M.tb* infection. (e) Treatment with anti-CXCR4 for 4 weeks revealed reduced necrotic area but deconstructed granuloma were evident. (f and g) Fractal analysis revealed the decreased necrotic area in the motixafortide-treated group with compacted granuloma which can be visually observed. (B) Necrotic area analysis was performed through ImageJ software. $^{***}P \leq 0.01$ vs. 6th week INF. All the images were captured through the same panel with MagVision software. *M. tb*, *Mycobacterium tuberculosis*; CXCR4, C-X-C motif chemokine receptor 4; RIF, rifampicin; INH, isoniazid.

the emergence of an acquired immune response. During the late stage of infection, multiple scattered areas were observed, resulting in the deconstructed granuloma following the spread of the infection via the deposition of debris in the airways (Fig. 5).

Anti-CXCR4 treatment reduces CD4⁺ T cell exhaustion. Because adaptation of anti-mycobacterial defence in the lungs is caused by immunological T-cell activation of macrophages (29), it is critical to investigate the role of anti-CXCR4 in the adaptive immune response. Significant

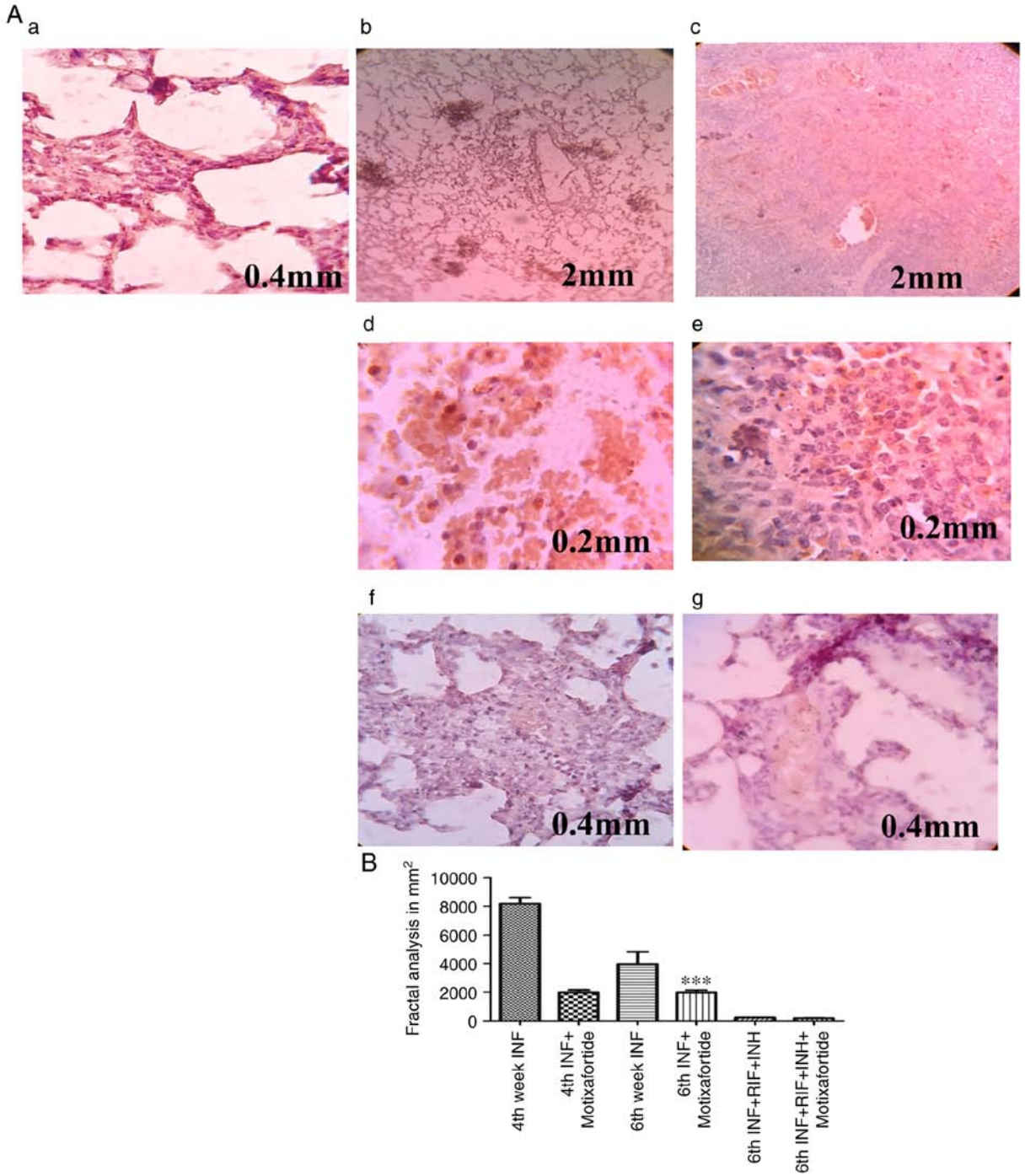

Figure 6. (A) DAB-stained sections of guinea pig lung tissues (magnification, x40). (a) Healthy guinea pig lung tissues. (b) The number of CD4+ T cells increased following *M.tb* infection in guinea pigs at the 4th week. (c) Following 2 weeks of motixafortide treatment in *M.tb*-infected guinea pigs, no marked changes were observed in the number of CD4+ T cells. (d) At the 6th week of *M.tb* infection in guinea pigs the number of CD4+ T cells decreased when compared with the 4th week infection. (e) Following 4 weeks of motixafortide treatment in *M.tb*-infected guinea pigs, no marked changes were observed in the number of CD4+ T cells. (f) Treatment with the anti-TB drugs revealed the marked changes in the number of CD4+ T cells when compared with the untreated guinea pigs. (g) Guinea pigs treated with anti-TB drugs along with motixafortide exhibited a marked reduction in the number of CD4+ T cells. (B) Bar chart showing the number of CD4+ T cells/unit area quanitified using ImageJ software. ***P≤0.01 vs. 6th week INF. *M. tb*, *Mycobacterium tuberculosis*; TB, tuberculosis; RIF, rifampicin; INH, isoniazid.

differences in the migration of CD4+ T cells to the granuloma site in *M.tb*-infected anti-CXCR4 treated guinea pigs and *M.tb*-infected guinea pigs during the early stages of TB infection were observed, indicating that excessive migration of T cells induces inflammation but has no effect on bacterial severity. During the 6th week, anti-CXCR4 used in conjunction with anti-TB medications decreased CD4+ T cells when compared to anti-TB drug therapy alone, indicating early bacterial load reduction (Fig. 6).

Discussion

CXCR4 signalling is necessary for the start of the granuloma-associated proangiogenic programme. Poor vascularization of the

developing granulomas in cxcr4b-deficient zebrafish embryos also inhibited bacterial growth. Since cxcr4b mutants shared similar microbicidal abilities against initial mycobacterial infection and shared a cellular composition with wild-type siblings in granulomatous lesions, the suppressed infection expansion in cxcr4b mutants could not be explained by a general lack of leukocyte recruitment or by a different intramacrophage bacterial growth rate (30). The expression of vegfaa was upregulated to a similar degree in cxcr4b mutants and wild-types, indicating that vascular endothelial growth factor is not required for the granuloma vascularization phenotype of cxcr4b mutants (30). Using anti-CXCR4 treatment in a guinea pig animal model, the function of the chemokine receptor CXCR4 in granuloma formation and the spread of mycobacterial infection was revealed. It was determined that inhibition of CXCR4 induced an attenuated infection, which could be related to pathogenic angiogenesis. The lungs sections were stained for $CD4^+$ T-cell expression to compare the difference in the number of lung T cells between anti-CXCR4-treated and *M.tb*-infected guinea pigs. The findings of the present study confirm the research that revealed that early TB spread of *M.tb* infection was associated with the onset of antimycobacterial immunity (31). The defect in the granuloma may be recapitulated by pharmacological inhibitors of CXCR4, such as motixafortide (BKT140 4-fluorobenzoyl) (32). Chemotaxis depends heavily on CXCR4. Additionally, the association between this receptor and angiogenesis is becoming more and more clear. Angiogenesis was recently discovered to be crucial for the growth of cellular clusters called granulomas, which contain the mycobacteria and are the hallmark of the TB disease, in the well-known zebrafish-*Mycobacterium marinum* (*M. marinum*) TB model. Supporting the study that CXCR4 induces angiogenesis, a positive association between the survival of mycobacteria and angiogenesis that is normally observed in *M.tb*-infected guinea pigs was restricted in anti-CXCR4-treated guinea pigs. A pharmacological antagonist of VEGFR has been proposed as a host-targeted therapy to suppress the formation of granulomas in TB patients (33). Based on the data of the present study, CXCR4 antagonists may be a novel adjunct combined with anti-TB drugs acting as anti-angiogenic TB therapy. The results indicate a role of CXCR4 in eliciting angiogenesis and inducing VEGF expression. Adaptation of anti-mycobacterial defence in the lungs is due to the activation of macrophages by immune T cells. Thus, it is important to analyse the involvement of anti-CXCR4 in the adaptive immune response, which was not addressed in the present study and is a limitation. Direct target or complete inhibition of such host factors may reveal an adverse effect in spite of decreasing disease progression. Inflammatory chemokines CCL2 and CXCL5 were suppressed and classical complement pathway factors were activated following dexamethasone treatment, while the effects were absent with anti-VEGF treatment (34). The CXCR4/CXCL12 axis has been revealed to induce tumour progression and angiogenesis by activating the PI3K/Akt pathway, resulting in increased expression of VEGF (35). VEGFR inhibitors act as extensive angiogenesis blockers, involving the generation of small vessels from inter-segmental vessels. CXCR4 exhaustion uniquely inhibits granuloma-induced angiogenesis (36). The significance of inflammation in triggering granuloma-induced angiogenesis and the exact mechanisms through which CXCR4 regulates new blood vessel formation requires further elucidation. Notably, the results also suggest that pathogenic angiogenesis may contain the dispersion of inflammation. In addition, CXCR4 inhibition or VEGF signalling attenuation has been revealed to lead to the formation of constructed granuloma and to reduce granuloma expansion (37). Infected miR-206-knockdown zebrafish embryos exhibited upregulation of cxcl12a and cxcr4b, and enhanced neutrophil recruitment to infection sites. Increased neutrophil response and decreased bacterial burden brought on by miR-206 knockdown depended on the Cxcl12/Cxcr4 signalling axis using CRISPR/Cas9-mediated knockdown of cxcl12a and cxcr4b expression and AMD3100 inhibition of Cxcr4 (38). Necrosis is induced by bacterial lysis and forms at the centre of the granuloma, resulting in the spreading of the infection and destruction of the lung tissue. Extracellular bacilli could be found in the necrotic region and released to the luminal side of the cavity, resulting in the spread of the infection (39). The inefficiency and long-term treatment strategy of anti-TB drugs are considered to be sources of pharmacokinetic factors (40). Aside from the complex array of diseased sites, the vasculature within granuloma impedes drug delivery (41). According to a previous study, CXCR4 has been linked to tumour angiogenesis via transcriptional regulation of VEGF signalling (42). It has been shown that *M. marinum* infection stimulates angiogenesis in zebrafish and supports the spread of bacterial infection (6). To verify the role of CXCR4 in dissemination of tuberculosis infection in guinea pigs, infected guinea pigs were injected with motixafortide subcutaneously thrice per week for 2 weeks after the established infection with the *M.tb* H37Rv strain, and VEGF expression was observed. Chemokines serve a critical function in directing immune cells to the inflammatory site, which may lead to unregulated angiogenesis and could be decisive in controlling the disease severity (43). In this regard, it is important to study the regulatory mechanisms involved in the production of chemokines linked with increased angiogenesis. The members of the CXC chemokine family that contain the ELR motif, as compared with those that lack these three amino acids, are potent inducers of angiogenic activity. When the concentration of anti-TB drugs was delineated in relation to the vascular density at the granuloma site, a steep gradient of reduced drug levels was found with increased vasculature. The restricted permeability of anti-TB drugs leads to drug tolerance that is associated with latent bacterial populations. Extensive drug distribution profiling should be considered during drug discovery to optimise drug penetration to infection sites such as granuloma and lesions. To reach the bacilli inside the macrophages, anti-TB drugs should be distributed into various parts by overcoming barriers such as lesions in the lungs with higher cellular composition and vascularization. From the blood, the drug enters into the interstitial space of lesions and then penetrates. In the present study it was demonstrated that the distribution of drug concentration decreased in the plasma, lungs, and granuloma, respectively. A limited number of animals was also a limitation of the present study. In the present study, inhibition of CXCR4 affected the expression of VEGFA and granuloma vascularisation. It was revealed that CXCR4 induced new blood vessel formation during TB infection. Obstruction of pathological angiogenesis with CXCR4 inhibitors is an alternative therapeutic strategy to normalise the vasculature at granuloma sites to increase the penetration of drugs, and reduce the bacterial count in the lungs. The pivotal step in preventing

drug resistance in TB and curing this disease may be achieved through efficient combination therapy, which distributes the drug into the lesion and lesion compartments targeting the vulnerable bacterial population.

Acknowledgements

We would like to thank Mr Nilesh Pal (Animal Experimentation Laboratory; ICMR-NJIL & OMD, Agra, India), and Mr Amit Kumar Rajput (Technician-C, Animal Experimentation Laboratory; ICMR-NJIL & OMD) for technical assistance.

Funding

The present study was supported by the Department of Science and Technology (DST), Government of India (New Delhi, India), DST-INSPIRE Fellowship (no. DST/INSPIRE Fellowship/2018/IF180175) awarded to KSD.

Availability of data and materials

The datasets used during the present study are available from the corresponding author upon reasonable request.

Authors' contributions

KSD and AKS conceived the study, analysed the data and wrote the manuscript. KSD and DSC designed the study. VK, AVS and SVS participated in data analysis. KSD and DSC confirm the authenticity of all the raw data. All the authors read and approved the final version of the manuscript.

Ethics approval and consent to participate

All the animal experimental methods described in the present study were conducted according to the relevant guidelines and regulations for handling laboratory animals and were approved (approval no. NJIL&OMD-3-IAEC/2019-08) by the Institutional Animal Ethics Committee of NJIL & OMD (Agra, India).

Patient consent for publication

Not applicable.

Competing interests

The authors declare that they have no competing interests.

References

1. WHO report 2019, https://apps.who.int/iris/bitstream/handle/10665/329368/9789241565714-eng.pdf
2. Polena H, Boudou F, Tilleul S, Dubois-Colas N, Lecointe C, Rakotosamimanana N, Pelizzola M, Andriamandimby SF, Raharimanga V, Charles P, *et al*: Mycobacterium tuberculosis exploits the formation of new blood vessels for its dissemination. Sci Rep 6: 33162, 2016.
3. Golden MP and Vikram HR: Extrapulmonary tuberculosis: An overview. Am Fam Physician 72: 1761-1768, 2005.
4. Russell DG, Barry CE III and Flynn JL: Tuberculosis: What we don't know can, and does, hurt us. Science 328: 852-856, 2010.
5. Dartois V: The path of anti-tuberculosis drugs: From blood to lesions to mycobacterial cells. Nat Rev Microbiol 12: 159-167, 2014.
6. Oehlers SH, Cronan MR, Scott NR, Thomas MI, Okuda KS, Walton EM, Beerman RW, Crosier PS and Tobin DM: Interception of host angiogenic signalling limits mycobacterial growth. Nature 517: 612-615, 2015.
7. Dvorak HF, Brown LF, Detmar M and Dvorak AM: Vascular permeability factor/vascular endothelial growth factor, microvascular hyperpermeability, and angiogenesis. Am J Pathol 146: 1029-1039, 1995.
8. Jain RK: Normalizing tumor vasculature with anti-angiogenic therapy: A new paradigm for combination therapy. Nat Med 7: 987-989, 2001.
9. Chackerian AA, Alt JM, Perera TV, Dascher CC and Behar SM: Dissemination of Mycobacterium tuberculosis is influenced by host factors and precedes the initiation of T-cell immunity. Infect Immun 70: 4501-4509, 2002.
10. Davis JM and Ramakrishnan L: The role of the granuloma in expansion and dissemination of early tuberculous infection. Cell 136: 37-49, 2009.
11. Monin L and Khader SA: Chemokines in tuberculosis: The good, the bad and the ugly. Semin Immunol 26: 552-558, 2014.
12. Keeley EC, Mehrad B and Strieter RM: Chemokines as mediators of neovascularization. Arterioscler Thromb Vasc Biol 28: 1928-1936, 2008.
13. Perez AL, Bachrach E, Illigens BM, Jun SJ, Bagden E, Steffen L, Flint A, McGowan FX, Del Nido P, Montecino-Rodriguez E, *et al*: CXCR4 enhances engraftment of muscle progenitor cells. Muscle Nerve 40: 562-572, 2009.
14. Hoshino Y, Tse DB, Rochford G, Prabhakar S, Hoshino S, Chitkara N, Kuwabara K, Ching E, Raju B, Gold JA, *et al*: Mycobacterium tuberculosis-induced CXCR4 and chemokine expression leads to preferential X4 HIV-1 replication in human macrophages. J Immunol 172: 6251-6258, 2004.
15. García-Cuesta EM, Santiago CA, Vallejo-Díaz J, Juarranz Y, Rodríguez-Frade JM and Mellado M: The role of the CXCL12/CXCR4/ACKR3 axis in autoimmune diseases. Front Endocrinol (Lausanne) 10: 585, 2019.
16. Gil M, Seshadri M, Komorowski MP, Abrams SI and Kozbor D: Targeting CXCL12/CXCR4 signaling with oncolytic virotherapy disrupts tumor vasculature and inhibits breast cancer metastases. Proc Natl Acad Sci USA 110: E1291-E1300, 2013.
17. Peled A, Abraham M, Avivi I, Rowe JM, Beider K, Wald H, Tiomkin L, Ribakovsky L, Riback Y, Ramati Y, *et al*: The high-affinity CXCR4 antagonist BKT140 is safe and induces a robust mobilization of human CD34+ cells in patients with multiple myeloma. Clin Cancer Res 20: 469-479, 2014.
18. Beider K, Begin M, Abraham M, Wald H, Weiss ID, Wald O, Pikarsky E, Zeira E, Eizenberg O, Galun E, *et al*: CXCR4 antagonist 4F-benzoyl-TN14003 inhibits leukemia and multiple myeloma tumor growth. Exp Hematol 39: 282-292, 2011.
19. Salcedo R, Wasserman K, Young HA, Grimm MC, Howard OM, Anver MR, Kleinman HK, Murphy WJ and Oppenheim JJ: Vascular endothelial growth factor and basic fibroblast growth factor induce expression of CXCR4 on human endothelial cells: In vivo neovascularization induced by stromal-derived factor-1alpha. Am J Pathol 154: 1125-1135, 1999.
20. Davuluri KS, Singh AK, Kumar V, Singh SV, Singh AV, Kumar S, Yadav R, Kushwaha S and Chauhan DS: Stimulated expression of ELR+ chemokines, VEGFA and TNF-AIP3 promote mycobacterial dissemination in extrapulmonary tuberculosis patients and Cavia porcellus model of tuberculosis. Tuberculosis (Edinb) 135: 102224, 2022.
21. Klinkenberg LG, Lee JH, Bishai WR and Karakousis PC: The stringent response is required for full virulence of Mycobacterium tuberculosis in guinea pigs. J Infect Dis 202: 1397-1404, 2010.
22. National Research Council (US) Committee for the Update of the Guide for the Care and Use of Laboratory Animals. Guide for the care and use of laboratory animals. 8th edition. Washington (DC): National Academies Press (US), 2011.
23. Kashino SS, Napolitano DR, Skobe Z and Campos-Neto A: Guinea pig model of Mycobacterium tuberculosis latent/dormant infection. Microbes Infect 10: 1469-1476, 2008.
24. Fischer AH, Jacobson KA, Rose J and Zeller R: Hematoxylin and eosin staining of tissue and cell sections. CSH Protoc 2008: pdb.prot4986, 2008.
25. Livak KJ and Schmittgen TD: Analysis of relative gene expression data using real-time quantitative PCR and the 2(-Delta Delta C(T)) method. Methods 25: 402-408, 2001.
26. Kim SW, Roh J and Park CS: Immunohistochemistry for pathologists: Protocols, pitfalls, and tips. J Pathol Transl Med 50: 411-418, 2016.

27. Goutal S, Auvity S, Legrand T, Hauquier F, Cisternino S, Chapy H, Saba W and Tournier N: Validation of a simple HPLC-UV method for rifampicin determination in plasma: Application to the study of rifampicin arteriovenous concentration gradient. J Pharm Biomed Anal 123: 173-178, 2016.
28. Aït Moussa L, El Bouazzi O, Serragui S, Soussi Tanani D, Soulaymani A and Soulaymani R: Rifampicin and isoniazid plasma concentrations in relation to adverse reactions in tuberculosis patients: A retrospective analysis. Ther Adv Drug Saf 7: 239-247, 2016.
29. Sia JK and Rengarajan J: Immunology of Mycobacterium tuberculosis Infections. Microbiol Spectr 7: 10.1128/microbiolspec.GPP3-0022-2018, 2019.
30. Torraca V, Tulotta C, Snaar-Jagalska BE and Meijer AH: The chemokine receptor CXCR4 promotes granuloma formation by sustaining a mycobacteria-induced angiogenesis programme. Sci Rep 7: 45061, 2017.
31. Ramonell KM, Zhang W, Hadley A, Chen CW, Fay KT, Lyons JD, Klingensmith NJ, McConnell KW, Coopersmith CM and Ford ML: CXCR4 blockade decreases CD4+ T cell exhaustion and improves survival in a murine model of polymicrobial sepsis. PLoS One 12: e0188882, 2017.
32. Reyes AWB, Arayan LT, Huy TXN, Vu SH, Kang CK, Min W, Lee HJ, Lee JH and Kim S: Chemokine receptor 4 (CXCR4) blockade enhances resistance to bacterial internalization in RAW264.7 cells and AMD3100, a CXCR4 antagonist, attenuates susceptibility to Brucella abortus 544 infection in a murine model. Vet Microbiol 237: 108402, 2019.
33. Pozzobon T, Goldoni G, Viola A and Molon B: CXCR4 signaling in health and disease. Immunol Lett 177: 6-15, 2016.
34. Mirabelli P, Mukwaya A, Lennikov A, Xeroudaki M, Peebo B, Schaupper M and Lagali N: Genome-wide expression differences in anti-Vegf and dexamethasone treatment of inflammatory angiogenesis in the rat cornea. Sci Rep 7: 7616, 2017.
35. Mousavi A: CXCL12/CXCR4 signal transduction in diseases and its molecular approaches in targeted-therapy. Immunol Lett 217: 91-115, 2020.
36. Liang Z, Brooks J, Willard M, Liang K, Yoon Y, Kang S and Shim H: CXCR4/CXCL12 axis promotes VEGF-mediated tumor angiogenesis through Akt signaling pathway. Biochem Biophys Res Commun 359: 716-722, 2007.
37. Kawaguchi N, Zhang TT and Nakanishi T: Involvement of CXCR4 in normal and abnormal development. Cells 8: 185, 2019.
38. Wright K, de Silva K, Plain KM, Purdie AC, Blair TA, Duggin IG, Britton WJ and Oehlers SH: Mycobacterial infection-induced miR-206 inhibits protective neutrophil recruitment via the CXCL12/CXCR4 signalling axis. PLoS Pathog 17: e1009186, 2021.
39. Philips JA and Ernst JD: Tuberculosis pathogenesis and immunity. Annu Rev Pathol 7: 353-384, 2012.
40. Xu Y, Wu J, Liao S and Sun Z: Treating tuberculosis with high doses of anti-TB drugs: Mechanisms and outcomes. Ann Clin Microbiol Antimicrob 16: 67, 2017.
41. Viaggi B, Cangialosi A, Langer M, Olivieri C, Gori A, Corona A, Finazzi S and Di Paolo A: Tissue penetration of antimicrobials in intensive care unit patients: A systematic review-part II. Antibiotics (Basel) 11: 1193, 2022.
42. Tong RT, Boucher Y, Kozin SV, Winkler F, Hicklin DJ and Jain RK: Vascular normalization by vascular endothelial growth factor receptor 2 blockade induces a pressure gradient across the vasculature and improves drug penetration in tumors. Cancer Res 64: 3731-3736, 2004.
43. Mehrad B, Keane MP and Strieter RM: Chemokines as mediators of angiogenesis. Thromb Haemost 97: 755-762, 2007.